Check for updates

The significance of growth shells in development of symmetry, transparency, and refraction of the human lens

Teri M. Greiling[1], Judy M. Clark[2] and John I. Clark[2,3]*

[1]Department of Dermatology, School of Medicine, Oregon Health & Science University, Portland, OR, United States, [2]Department of Biological Structure, University of Washington, Seattle, WA, United States, [3]Department of Biological Structure & Ophthalmology, School of Medicine, University of Washington, Seattle, WA, United States

Human visual function depends on the biological lens, a biconvex optical element formed by coordinated, synchronous generation of growth shells produced from ordered cells at the lens equator, the distal edge of the epithelium. Growth shells are comprised of straight (St) and S-shaped (SSh) lens fibers organized in highly symmetric, sinusoidal pattern which optimizes both the refractile, transparent structure and the unique microcirculation that regulates hydration and nutrition over the lifetime of an individual. The fiber cells are characterized by diversity in composition and age. All fiber cells remain interconnected in their growth shells throughout the life of the adult lens. As an optical element, cellular differentiation is constrained by the physical properties of light and its special development accounts for its characteristic symmetry, gradient of refractive index (GRIN), short range transparent order (SRO), and functional longevity. The complex sinusoidal structure is the basis for the lens microcirculation required for the establishment and maintenance of image formation.

KEYWORDS

lens development, growth shells, symmetry, transparency, refraction, microcirculation

Introduction

Symmetry, refraction and transparency are optical properties of the biological lens required for image formation in the human eye. Studies of lens growth and development across species report that exponential growth is continuous throughout life without loss or replacement of cells. A typical model for exponential growth is: $W = Wm\ e^{-k/A}$ (where "W" is dry weight, "Wm" = maximum weight, "k" is rate of growth, and "A" is postnatal age) ([1], [2]). Lens dimensions increase synchronously and continuously through the addition of symmetric growth shells. These growth shells form a complex sinusoidal structure that

forms the basis for the lens microcirculation and the formation and maintenance of transparency.

Brief summary of lens embryology

Lens placode

At ~3 weeks of gestation in humans, a small number of cells (50 to 100) swell, thicken, and form a lens placode at the edge of the neural plate (neuroectoderm). This lens placode is the origin of the cells that generate the refractile, symmetric, transparent lens (Figure 1). The cells in cranial placodes resemble neural progenitors that differentiate into sensory neurons characterized by cytoskeleton-enriched processes, forming dendrites and axons, extending from a cell body containing a nucleus and plentiful organelles to support cell-to-cell connectivity (3–7). In contrast to cells in the sensory placodes, cells in the lens placode swell, thicken and invaginate to form a fluid-filled lens vesicle superficial to the developing optic cup (future retina) (Figure 2) (3, 8–11).

Lens vesicle becomes the lens nucleus

Elongation of the posterior cells in the lens vesicle closest to the optic cup results in a solid cellular mass with the apical surfaces facing inward and the basal surfaces outward. The intercellular space is compressed, and these cells become the "primary" fibers of the "embryonic nucleus", supplied temporarily by the hyaloid artery, a branch of the ophthalmic artery to the optic cup (2, 3,

FIGURE 1
CRANIAL PLACODES in the TRILAMINAR EMBRYO. This figure represents a dorsal view of the ectodermal surface of a trilaminar embryo, prior to neural tube formation (K. Altdorfer, https://slideplayer.com/slide/12872844/). As the neural plate forms, a horseshoe shaped region peripheral to the cranial end of the neural ectoderm, called pre-placodal ectoderm (PPE), forms localized thickenings, "cranial placodes", for specialized structures including the lens. A number of cranial placodes are indicated by circles and labeled. The lens placode responds to signaling pathways involving FGF, BMP, Notch, Wnt, betacatenin, and others described elsewhere in the text.

11, 12). The anterior cells of the lens vesicle distal to the optic cup are not induced to elongate and remain an epithelial monolayer covering the anterior surface of the embryonic nucleus, and the germinative center for future growth shells (Figure 2). (NOTE ABOUT TERMINOLOGY: Early studies suggested the lens was a single giant cell, with a pale yellow nucleus at the core, surrounded by a clear albuminoid cortex, like an egg. When the lens was confirmed to be a cellular tissue, use of the terminology "cortex" and "nucleus" continued to describe cells in the lens periphery and lens center, respectively (13, 14).

First growth shells

The cells in the anterior epithelial layer can proliferate and migrate toward the equator of the developing lens, where they organize into ordered meridional rows. Synchronized elongation of the meridional cells, posteriorly and anteriorly, initiates the formation of a coordinated band of arc-shaped secondary cells, parallel to the optic axis. This band will become a growth shell at the peripheral lens cortex (Figure 3) (2, 9, 11, 15, 16). As the temporary vessels of the hyaloid vasculature regress, each growth shell becomes the developmental mechanism for adding symmetric layers of new "secondary" fibers that increase the size of the lens during formation of the visual system (Figure 2). New growth shells contain malleable, refractile, organelle-free secondary fibers that subsume previous shells surrounding the lens nucleus (17–20). New growth shells can adjust to the optical needs of a growing eye (16, 21).

It is important to emphasize that the coordinated addition of symmetric growth shells of secondary fibers expands the size of the lens and creates a biconvex, biological spheroid that functions as an optical element in the human eye (Figure 4) (11, 19, 22–24). The spheroid is defined by an equator separating the anterior from the posterior hemisphere. The radius of curvature of the surface anterior to the lens equator is ~10mm and the radius of curvature of the surface posterior to the equator is ~6mm (see Figure 2) (25, 26). With the growth of the visual system, the optical curvatures vary slightly as they adjust the focal length of the lens to the dimensions of the changing eye (16, 27). Throughout development of visual function, the optics of the growing lens are carefully synchronized with the establishment and maintenance of optical quality during the life of an individual (16, 22, 28). As a mechanism for the development of optics, growth shells are an unprecedented success.

Cellular specialization

In the absence of blood vessels, each growth shell develops symmetric layers of cellular fibers, containing condensed cytoplasmic proteins, largely crystallins and cytoskeleton, to increase the refractive index, and establish transparent short-range order necessary for focusing images on the retina (3, 22, 29). Growth shells can do more. Without blood vessels, structural specializations in the fibers of growth shells contribute to a symmetric circulatory system for fluid flow that regulates hydration, ionic homeostasis, and uniform distribution of nutrients, in support of dynamic growth to
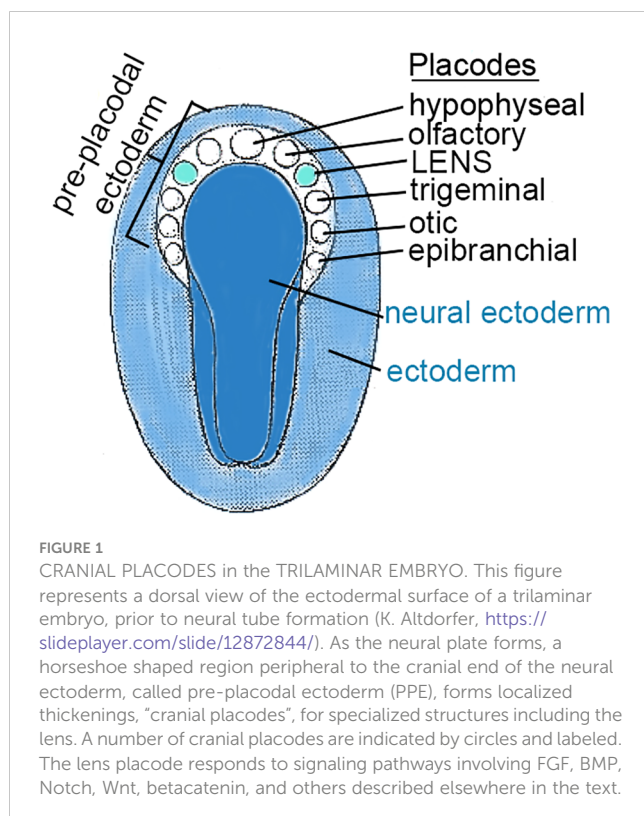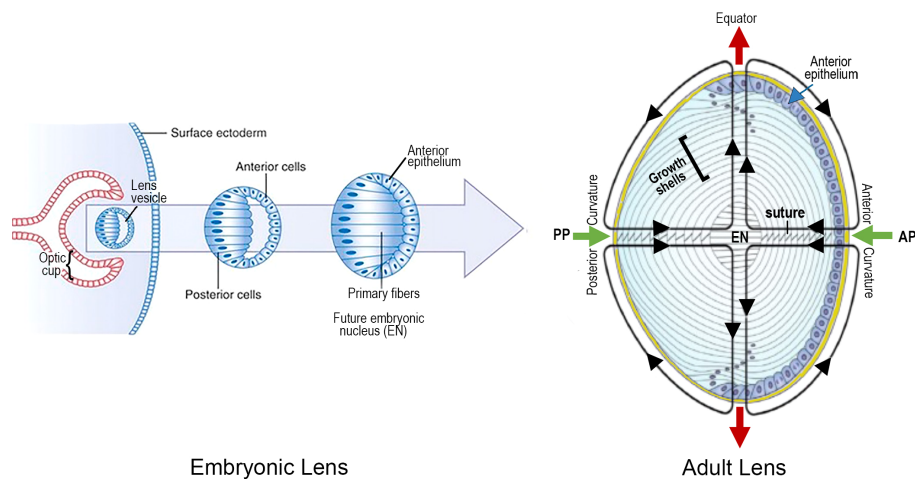
FIGURE 2
LENS DEVELOPMENT is a MULTISTEP PROCESS BEGINNING at ~3 to 4 WEEKS of EMBRYONIC AGE in the HUMAN: An optic cup extends toward the surface ectoderm from the neural tube, deep to the lens placode. The optic cup induces invagination of the lens placode, followed by its separation from the surface as the lens vesicle. Hyaloid vessels (not shown) supply the developing lens briefly, before regressing. Maturation of the lens vesicle is accompanied by lengthening of the posterior lens cells, adjacent to the optic cup, to form "primary lens fibers". These cells lose their nuclei and close the vesicle to create a solid cellular mass. In contrast, the anterior cells become an anterior epithelium that maintains its proliferative ability. Synchronous proliferation, migration and elongation of waves of epithelial cells generate "secondary" lens fibers that form growth shells. The growth shells surround the primary fibers of the "embryonic nucleus" (EN), to expand the size of the lens as the optics adjust to the growing eye. The entire lens mass develops within a thick basement membrane capsule (thick yellow line). An adult lens is refractile, transparent and biconvex, consisting of concentric layers of lens fiber growth shells. The functional viability and plasticity of an adult lens is prolonged through a unique microcirculation that nourishes, hydrates and maintains normal electrophysiological homeostasis as the lens grows and adjusts to the optical needs of the growing retina. The image on the right summarizes the microcirculation: Green arrows indicate the inflow of fluid at the anterior (AP) and posterior (PP) poles at the center of the anterior and posterior curvatures. Red arrows represent the fluid outflow at the equator. A number of growth factor pathways are essential for regulation during both embryogenesis and growth shell formation.

optimize the optics for the growing, changing visual system (Figure 2) (3, 7, 12, 30, 31). Without a functioning microcirculation, the lens cannot develop the symmetric gradient of refractive index (GRIN) and transparency required for image formation in the growing visual system (32–35). In fact, the lens might as well be a piece of glass or plastic. Instead, nature created a growth shell mechanism for the biological lens, that is unique in all of developmental biology (36, 37).

Growth shells

Structure: straight and S-shaped fibers

Each growth shell is comprised of two types of secondary fibers: straight (St) and S-shaped (SSh) fibers (Figure 4) (22, 36). St fibers are crescent-shaped, parallel to the visual axis, and attached to either the posterior or anterior pole (Figures 4A, B), where they become growth centers for the anterior or posterior hemispheres of the growth shell. Posterior to the lens equator, St fibers radiate away from the posterior pole, separated by 120 degrees (Figure 4B) and anterior to the lens equator, St fibers radiate away from the anterior pole separated by 120 degrees (Figure 4B). Notice that the tips of the elongating St fibers stop short of the opposite poles, ending at the tips of the Y suture (Figure 4B) (15, 22, 38).

The second type of lens fibers, the SSh fibers, fill in the growth shell (Figure 4A). SSh fibers are oriented along, and adjacent to, the St fibers (Figures 4A, B). SSh fibers have three parts: a straight middle segment, parallel to the St fiber, and two tips, curving away

from the St fiber, to meet curved tips from other SSh fibers forming a pair of SSh fibers (Figure 4, red fibers). Anterior to the equator, where the curved tips meet, the anterior suture forms, and posterior to the equator, where the curved tips meet, the posterior suture forms. The sutures are formed where pairs of SSh fibers meet, anteriorly or posteriorly (Figure 4, red fibers). Because the tips curve to meet other SSh fibers, they appear as symmetric, sigmoid-shaped fiber cells when projected in 2-D (Figure 4D). The trigonometric function describing the SSh fiber is f(x) = arctan(x), which is the basis for the symmetry of a growth shell and accounts for the symmetric index of refraction, transparency, and the anterior and posterior curvatures of the lens.

Structure: sinusoidal networks form Y sutures

Where the curved tips meet anteriorly, the sutures are positioned in a "Y-shape" and posteriorly, the sutures form an "inverted Y-shape" (22). The anterior and posterior sutures are not aligned and are offset by 60 degrees. This is because of the sigmoid shape of SSh fibers (Figure 4D). Because the SSh tips curve in opposite directions away from their middle (Figure 4C), they are no longer in the same anterior/posterior plane (22, 37–39). Still, symmetry is maintained in normal development. The result is a continuous, interconnected sinusoidal network of fibers throughout the entire growth shell. Throughout the growth shell, SSh fibers in the posterior hemisphere connect directly with the fibers in the
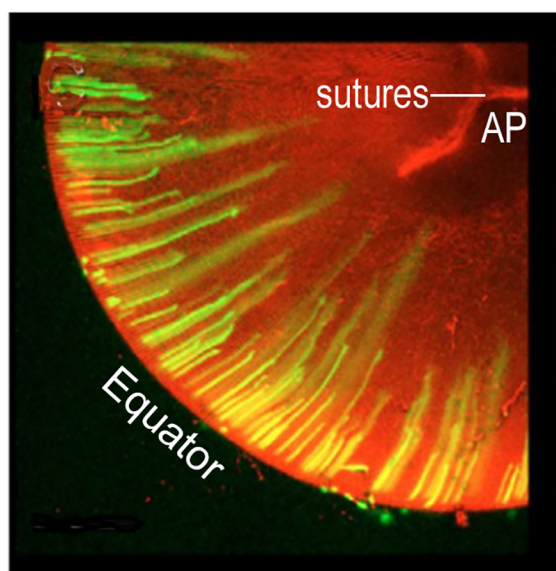
FIGURE 3
GROWTH SHELL FORMATION BEGINS WITH COORDINATED, PERIODIC ELONGATION of EPITHELIAL CELLS at the EQUATOR. Initially, anterior and posterior elongation of lens epithelial cells produces straight segments that form a discontinuous band around the lens periphery. In this image, green fluorescent protein, GFP, labels the cells elongating away from the equator. With continued elongation, a small number of these fibers will attach at the anterior (AP) or posterior (PP) poles separated radially by ~120 deg, (2.09 radians) (not shown). These are the straight (St) fibers that orient all other cells to fill in the growth shell. The optic axis (not shown) connects the AP with the PP. Elongation is synchronous and coordinated. In the figure, the longer fibers are believed to be forming one growth shell and the shorter fibers are beginning to elongate to form the next growth shell. Growth shells form concentric layers observed in intact lenses. (modified from Shi et al. (2009) J. Cell Sci. 122:1607-15).

anterior hemisphere. It is easy to understand how reactive oxygen species, advanced glycation end products, inflammatory agents, osmolytes, or other systemic stresses can disrupt the coordinated, symmetric elongation of fibers and alter the suture patterns.

Careful analysis of electron micrographs of developing lenses confirms that sutures in a growth shell are formed by the connections between differentiating SSh fibers (22, 36, 38–40). In contrast, the embryonic lens nucleus at the center of the adult lens has no sutures and consists of the primary fibers that elongated to obliterate the lens vesicle and establish the original cell mass (Figure 2). Subsequently the embryonic nucleus is overlain by secondary fibers (22, 38). As lens development continues, secondary fibers organize into isomorphic interconnected growth shells in a coordinated, synchronized process. The amount of curvature in the individual tips of the SSh fibers varies relative to position relative to where the pairs meet and establish a suture (Figure 4) (39). An unexpected result is the normal variability in the lengths of the SSh fibers connecting along the suture lines. The lengths oscillate with a regular, sinusoidal pattern, another indication of coordinated, synchronization of growth shell formation (Figure 5). It should be noted that the ends of secondary fibers expand and overlap at the sutures (39, 40).

The overlap is part of the 3-D interconnected suture planes, extending from the surface into the embryonic nucleus. The suture can act as a channel carrying fluid containing ions, nutrients, soluble factors, and antioxidants that regulate and maintain symmetric structure (7, 22, 41, 42). When normal fiber differentiation is disrupted, the sutures appear abnormal (22).

Structure modeling

When first observed, the unusual organization of St and SSh fibers is a bit confusing and difficult to understand. To visualize the details and the overall structure of a growth shell during development, growth, and aging, Kuszak chose 2-D projections (22, 36–38, 40). Using computer aided drawings, he applied geometric methods known since Babylonian times for navigation of the earth (a spheroid) to study fiber patterns in growth shells of the biological lens (also a spheroid) (Figure 6) (22, 38). Combining computer aided drawing with thorough, careful scanning electron microscopy, Kuszak revealed new information about the assembly of symmetric growth shells in the lens. His results represent the synchronous differentiation that is the structural basis for both the lens optics and the symmetric microcirculation of fluid throughout the lens, in the absence of vasculature. When differentiating fibers in the growth shells are exposed to fluid influx through posterior and anterior sutures, they can respond to the fluid contents like ions, nutrients, and soluble factors controlling lens growth. The extensive connectivity between SSh fibers in the growth shells, specifically posterior and anterior to the equator, accounts for the symmetry of the posterior and anterior curvatures of the developing lens. The importance of two organizing centers at the posterior and anterior poles is very clear. While growth shells were recognized previously in lens research, the 3-D computer aided drawing provides much greater detail about their symmetric structure and, potentially, their functional significance. The collective interactions between component St and SSh fibers account for the connectivity and symmetry in the growth shells (22, 36, 37).

Function in microcirculation

Growth shell formation is not simply a space-filling exercise. It is the basis for a highly connected, complex cellular network, organized to provide maximal image quality to millions of photoreceptors in the visual system. Lens growth is carefully regulated to form a symmetric, refractive optical element that transmits light waves for the formation of accurate visual images (7, 31). It is often unappreciated that a lens consists of diverse populations of fibers constituted from various protein and membrane specializations completed at very different ages across the life of the organism. The process of growth shell formation is the foundation for the symmetry necessary to optimize optical quality, including the gradient of refractive index, GRIN, and transparency in a growing eye.

Many biologists accept the correlation between structure and function (11, 37, 40, 43, 44). As explained in the legend of Figure 6,
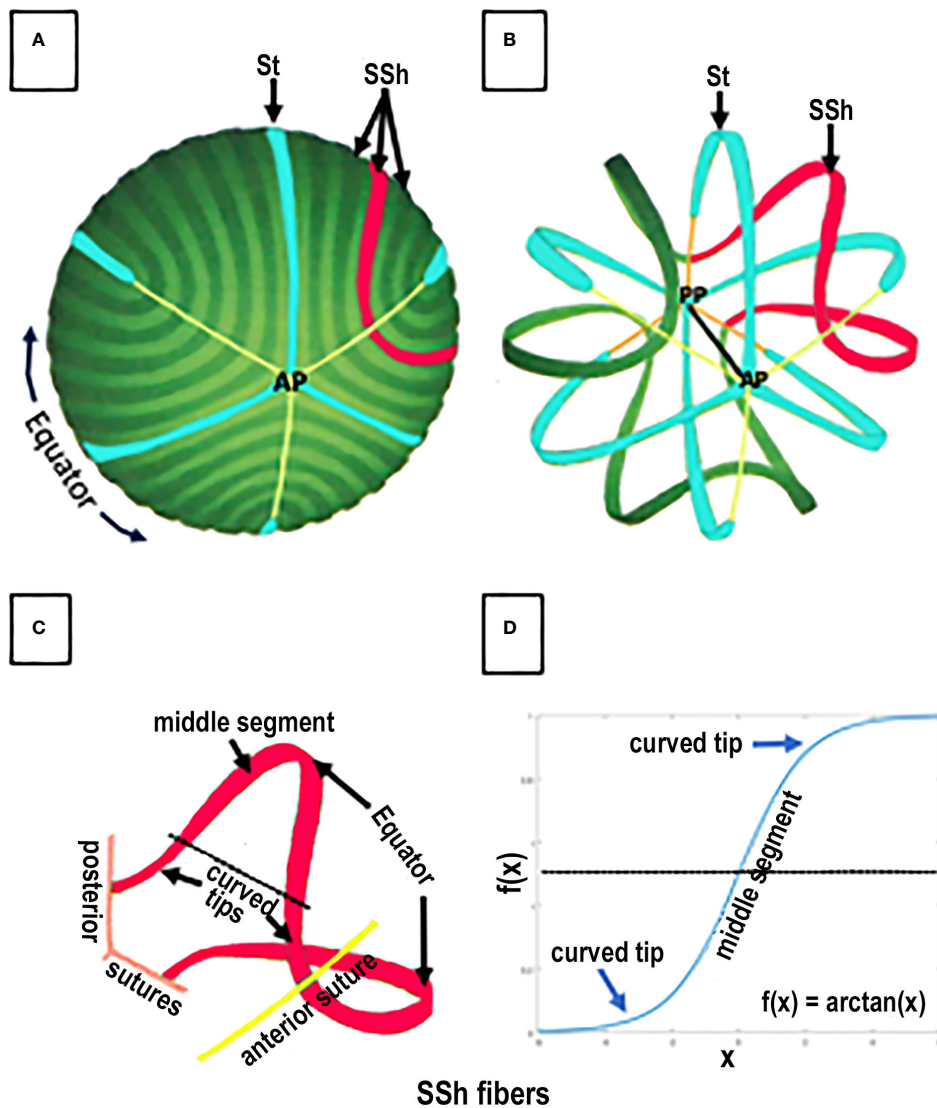
FIGURE 4

SPACE FILLING and FIBER ORGANIZATION in a GROWTH SHELL. An anterior view of the lens fibers in a typical GROWTH SHELL is shown in **(A)**. The dark and light green bands, each representing 20 individual fibers, are modeled from scanning electron micrographs of the growth shell surface. A few straight (St) fibers (turquoise) attaching at the anterior pole **(B)** are organizing centers for the many S-shaped (SSh) fibers (example highlighted in red) that fill-in the developing growth shell forming the anterior and posterior curvatures of each hemisphere in the biconvex lens **(A, B)**. Three sutures originating at the anterior (AP) poles are shown as thin yellow lines. Removing a number of fibers (in the figure) allows both the anterior (AP) and posterior (PP) poles to be seen **(B)** where three attachments for St fibers and three sutures (orange line) are shown. The optic axis (black line) connects the anterior and posterior poles. Space filling is a complex process of fiber assembly. During the start of fiber elongation, the middle segment of each SSh fiber is parallel to the optic axis (as in Figure 3). While one tip of an St fiber (blue) attaches at either the anterior (AP) or posterior (PP) pole, the other tip is the origin of the sutures **(A, B)** and the St fibers remain parallel to the optic axis. In contrast, the tips of elongating SSh fibers (red) do NOT attach at either pole. Instead, the elongating tips of SSh fibers curve away from the poles, toward the plane of the orienting St fibers, where they join the curved tips from a corresponding SSh fiber, to form a pair and create a suture **(B red)**. For example, **(C)** represents a pair of red SSh fibers. An anterior tip curves to meet the curved tip of an SSh fiber (red) elongating from the opposite side of the St fiber and form anterior (yellow) suture. Note that the SSh fibers are not attached at a pole and each new connection between the SSh fibers lengthens the suture. Similarly, the posterior tip of the same red SSh fiber curves to meet the tip of a corresponding SSh fiber (not shown) to form and lengthen the posterior suture **(C)**. Both sutures are shown in the figure, but the suture is only formed when the tips of each SSh pair connect. In this way pairs of elongating SSh fibers fill in a GROWTH SHELL as they establish the sutures. (NOTE about TERMINOLOGY: The SSh fibers are described as having "opposite end curvature" by Kuszak because they curve away from the St fibers and the poles. In a 2-D projection of an SSh fiber **(D)**, each SSh fiber can be described as having a distinctive symmetric, sigmoid shape with the two curved tips extending away from a straight middle segment **(D)**. The sigmoid function is defined as f(x) = arctan(x). It is well established, but not widely appreciated, that when SSh fibers meet other SSh fibers, the pairs of SSh fibers fill in and form the posterior and the anterior surface of a GROWTH SHELL. When SSh pairs connect, the sutures are formed. Altered sutures are an indication of abnormal lens fiber differentiation and function.
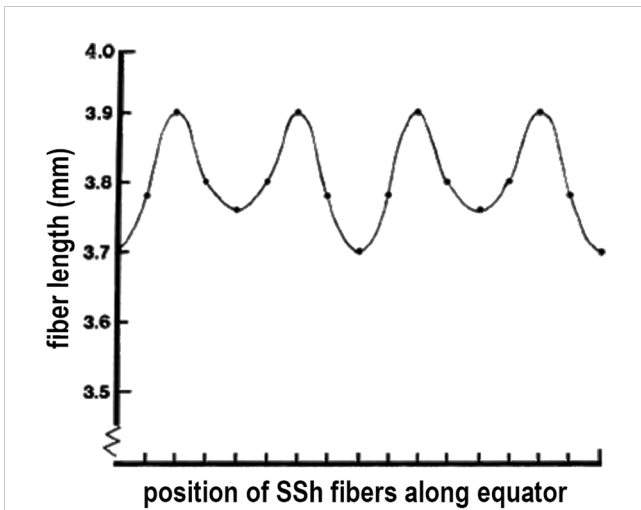
FIGURE 5
VARIATIONS in FIBER LENGTH in a GROWTH SHELL. Because the pairs of elongating SSh fibers intersect the equator, the length from the equator to fiber tip is expected to be unequal. When actually measured and plotted, an unexpected finding is that the variations in length are regular and periodic. Periodic oscillations in lens fiber lengths represent a sinusoidal pattern, reflecting the careful synchronization in growth shell formation.

the 2-D map of the growth shell introduces distortion at the anterior and posterior poles enlarging the dimension of the St fibers (Figure 6). Regardless of the distortion in a 2-D map, the regular, symmetric pattern of oscillating fibers posterior and anterior to the lens equator is expected to be critical for the growth shell mechanism of lens development (Figure 6) (22). The vertical clefts labeled "St" are the straight (St) fibers. Together with the sutures, St fibers are positioned every 60 degrees (1.05 radians) forming regular orienting centers for "waves" of SSh fibers (wavelength 120 degrees or 2.1 radians) above and below the equator (Figure 6). The periodic oscillations are oriented to the positions of the St fibers and sutures anteriorly and posteriorly. In the absence of vasculature, a simple hypothesis is that these sinusoidal oscillations are the structural basis for uniform symmetric fluid flow, known as microcirculation. If St fibers are spatial organizing centers for symmetric SSh fiber elongation, then the microcirculation can facilitate uniform fluid flow into the growth shells, anteriorly and posteriorly, to carry nutrients, growth factors, and protective molecules deep into the lens to organize and maintain function (Figure 2) (7, 42, 45). Recent studies report the importance of uniform, symmetric fluid flow in the control of hydration, ion homeostasis, refraction, and transparency in the biological lens (31, 32, 42, 45–47).
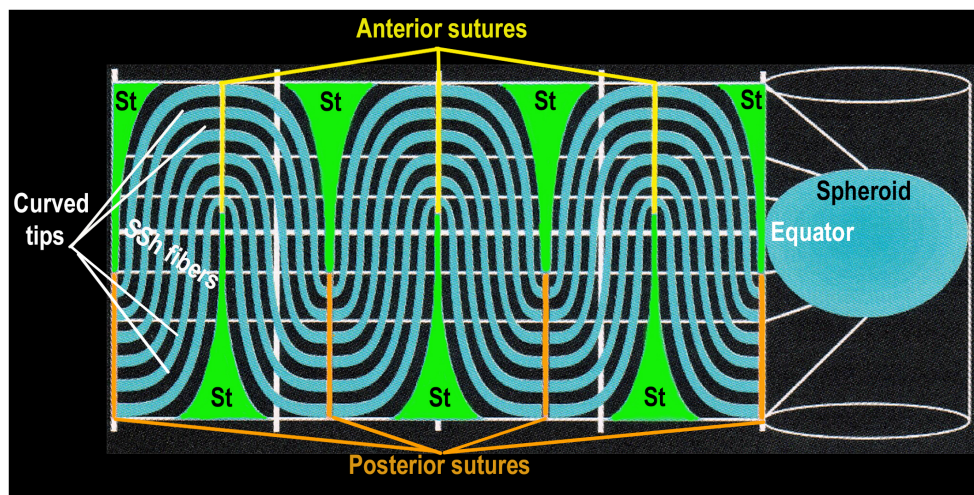

FIGURE 6
SYMMETRY is DETERMINED by TWO TYPES of DIFFERENTIATED FIBER CELLS. This is a 2-dimensional projection of a GROWTH SHELL. The computer aided drawing software generates a 2-D map by projecting the 3-D lens spheroid (growth shell) onto a 2-D cylindrical surface (Figure 6 right side). It is known as a projection because it simulates a bright light placed inside the spheroid so that any point (x,y,z) on the surface of the 3-D spheroid is projected to a point (x,y) on the surface of a cylindrical screen, surrounding the spheroid (Figure 6, right side). The lens equator is represented as a horizontal white line on the cylinder, between the anterior and posterior poles, represented as the open ends of the cylinder. When the computer "unfolds" the cylinder, the most obvious structural features of the 2-D projection of a typical growth shell are the symmetric oscillations of the SSh fibers (black and turquoise) above and below the equator (dashed white line), centered on the St fibers (green), positioned ~60 deg (1.05 radians) apart. The St fibers appear "cone shaped" with a wide base near the pole and a narrow tip at the beginning of each suture, near the equator. This distortion of St fiber dimensions is the result of an increase in scale near top and bottom of the cylinder, making the St fibers appear disproportionately large at the poles. (The St fibers are represented accurately in Figures 4A, B where their relative size is the same size as that observed *in situ* in electron micrographs of actual lenses.) In the 2-D map, the anterior sutures are represented by yellow vertical lines at the top of the 2-D map and the posterior sutures are orange vertical lines at the bottom of the 2-D map. Even though distorted, the St fibers extend from a pole to a tip of each suture near the equator (white line). The curved S-shaped (SSh) fibers form the oscillating pattern filling the growth shell. One curved tip of the SSh fibers connects to a posterior suture and the other curved tip connects to an anterior suture. The extensive fiber interconnections throughout the growth shell form a symmetric sinusoidal pattern essential for the organization of a symmetric microcirculation. This fiber symmetry is the basis for establishment and maintenance of refraction and transparency in an effective optical element in the human lens.

Few examples of symmetry in a biological tissue are more impressive than the experimental measurement of the loops of current flow in a biological lens (Figure 2) (46, 48–53). At the time it was reported, the significance of the symmetric current inflow and outflow in lens fiber symmetry and function was unrecognized (48, 53). Now, penetration of nutrients, metabolites, ions, and soluble factors is thought to occur through influx of fluid into the anterior and posterior suture planes, established by the alignment of sutures during the synchronized formation of growth shells (Figure 6). Fluid efflux occurs at the equator through an intercellular outflow pathway thought to be mediated by gap junctions. Hydrostatic pressure as high as 335 mm Hg centrally, falls to 0 mm Hg at the periphery, creating a pressure gradient for driving flow. The activity and localization of channels in the fiber membranes regulate flow and are critical for the optics of the visual system (7, 11, 31, 42, 45, 47, 50, 54).

There is much to learn from the lens about biological symmetry. The growth shell mechanism is a rare example of a developmental process for continuous formation and maintenance, year after year, of a highly symmetric refractile, transparent tissue, and the establishment of corresponding microcirculation. No other cellular tissue in the human compares with the transparent lens for studies of complex molecular and cellular function over a lifetime. Lens structure and function for image formation is intimately linked to symmetry, the gradient of refractive index (GRIN), and transparent short range order. In the eye, the dynamics of collective, often complex, interactions, at the molecular and cellular levels are accessible to modern, non-invasive methods of research in living individuals.

The current hypothesis that the microcirculation is a primary factor in the formation of the biconvex, human lens, places an emphasis directly on the significance of fiber membranes (45, 55–58). The 1000-fold elongation of the SSh secondary lens fibers is achieved through a dramatic expansion of the membrane surface area (22, 38, 59–63) accompanied by an elaborate reorganization of the lens fiber cytoskeleton (11, 60, 61, 64–69). It is well established that lens fiber membranes are specialized to facilitate fluid flow throughout the decreased intercellular spaces. During the formation of a growth shell the cytoskeleton condenses at the periphery of the hexagonal fibers, as a dramatic increase in the proportion of membrane cholesterol accompanies the increase in fiber membranes, and the intercellular spaces are narrowed (11, 70–75). Intuitively, a decrease in the extracellular space might be expected to increase resistance to fluid flow through the lens microcirculation. Studies of microfluidity suggest the opposite effect (76–79). High cholesterol can stabilize membranes, increase hydrophobicity to decrease surface tension, and help move fluids through the microcirculation of the lens (80). The complexity and heterogeneity of fiber membranes and their microenvironment make the study of microcirculation a challenge. While discussion of the origins of the microcirculation in the growth shell mechanism is beyond the scope of this article, growth shells are incredibly important as a foundation for development of the lens as an optical element in the human eye (58).

When the space between cell membranes decreases, the resistance to turbulent flow can decrease to favor laminar flow, increasing microfluidity (77, 79). The microfluidity between membranes can be enhanced further by an increase in the area of hydrophobic surface,

reducing interactions between aqueous fluid and charged membrane phospholipids (80). Increased membrane cholesterol resists oxygen permeability favoring elimination of intracellular organelles (81, 82) and stabilizes the elongated fiber shape, the condensation of the cytoskeleton at the cell periphery, the establishment of transparent short range order, phospholipid surface projections, and a decrease the intercellular spaces (83–85). A dynamic cytoskeleton compresses and stabilizes the cell membrane and positions membrane channels, cell adhesion molecules, and connexins along the cell surface. The constructive effects of high cholesterol levels in fiber membrane can contribute to lens microcirculation and improve symmetry, transparency, and GRIN in the lens as new symmetric growth shells are added (82, 84–86).

When growth shells are added at the lens periphery, they seem most responsive to constituents of the microcirculation. There appears to be a narrow band of growth shells forming a supranuclear region between the lens nucleus and cortex, where plasticity permits fiber reorganization (17, 87–90). Both electrophysiology and light scattering results indicate a subtle change several layers deep to the surface, consistent with an electrophysiological syncytium, and/or a network of interacting proteins and membranes (16, 17, 27, 90–92). Apparently, supranuclear fibers in new shells share plasticity to remodel the surface curvatures and adjust the biconvex lens to changes in optical requirements as the eye grows. The plasticity that accounts for variations in light scattering appears be sensitive to intracellular modifications associated with clinical conditions specific to light scattering phenotypes, including myotonic dystrophy, genetic mutations, Down Syndrome and Alzheimer's Disease (89, 93–95).

Plasticity of growth shells

Plasticity of the lens growth shells allows for subtle improvements in the optical properties as eyes grow from youth to adult (16, 96, 97). Developmentally, dramatic plasticity is demonstrated in lens inversion experiments (98, 99). After removal from the optic cup, a developing lens can be rotated 180 degrees, and then replaced in the eye so that the epithelium now faces the vitreous (posteriorly) instead of the aqueous (anteriorly). After replacement, repolarization occurs so that the (now) posterior epithelium elongates to fill-in the lens vesicle and a "cap" of new epithelium forms anteriorly facing the cornea. The results represent an extraordinary malleability that allows the newest growth shells to respond to factors carried through the microcirculation from the anterior aqueous and/or posterior vitreous. In a separate example of plasticity, a second lens mass develops in a mutant zebrafish, apparently because of two growth centers (100). One of the most extreme examples of lens plasticity during normal development is the lens of the "four-eyed" fish, Anablebs anableps (101–103). The two growth centers in the growth shells account for the formation of a pyriform-shaped lens that focuses light waves simultaneously, from two separate environments: air and water, onto separate regions of the same retina. In a 2-D map of a growth shell, individual SSh fibers are exposed to both the posterior and anterior environments by an influx of fluid carried through their posterior or anterior sutures (Figure 6). Lens fiber plasticity permits the posterior

and/or anterior curvatures to adjust refraction in response to either environment (posterior or anterior).

Each growth shell generates symmetric posterior and anterior convexities, with different radii of curvature, to adjust lens optics for precise focusing of images on a growing, expanding retina with minimal spherical aberration. Generation of two biconvex surfaces in the biological lens is achieved when posterior and anterior growth centers are established by the St fibers. Orientation of the SSh fibers, connecting at the sutures posteriorly and anteriorly, forms two biconvex surfaces that optimize the optics of the visual system. The number and orientation of lens fibers need to adjust the size of each new growth shell with age, to conform to the principles of image formation in the changing human eye (19, 22, 104).

Regulation of growth shell formation

Growth shell development is regulated largely by growth factor and signaling pathways involving FGF, BMP, IGF, TGFbeta, Notch, wnt, PDGF, and others (2, 3, 10, 23, 57, 105–112). Numerous studies support the hypothesis that concentration gradients of FGF and BMP are central to the regulation of elongation and maturation of lens fibers (14, 113). These are reviewed in detail elsewhere (10, 14). Both the levels of the growth factors in aqueous and vitreous and the locations of their receptors in the lens regulate formation of the symmetric growth shells (108, 111, 114, 115). The impact of these regulatory pathways on lens growth and differentiation is so important that there is systematic redundancy, so that IGF, EGF, TGFbeta, and other soluble factors contribute to formation of a growth shell. Redundancy benefits and protects the effectiveness of the growth shell mechanism in the formation of symmetric, concentric spherical layers. Given the complexities of the relationships between growth factors, signaling pathways and, gene regulatory networks on fiber differentiation, the importance of the synchronization of growth shell formation is sometimes overlooked. Bursts of transcription are a direct measure of the synchronized fiber differentiation in the coordinated development of the growth shells, and are necessary for generation of symmetry (10, 32, 116–118). The pulsatile activity of PDGF and the discovery of PDGF receptor in distal regions of lens epithelium where synchronicity is initiated, altered our understanding of the regulation of periodic symmetry in the biological lens (106, 119–123). Correlation of the cellular distributions of growth factors and receptors will clarify the link between growth factor activity and coordination of the remarkable geometric patterns (Figure 6) accounting for symmetry, GRIN, and transparent short range order in the biological lens.

Research continues to demonstrate the importance of synchronization of growth factors in regulating development and maintenance of symmetry, GRIN, and transparency in the biological lens (2, 10, 105, 106, 109–113, 119–122, 124–126). Differentiation of symmetric, concentric layers of elongated, denucleated, transparent, refractile fiber cells in the lens spheroid is complex and represents unprecedented spatio-temporal regulation in biology (11, 22, 37, 38, 121). Although the lens
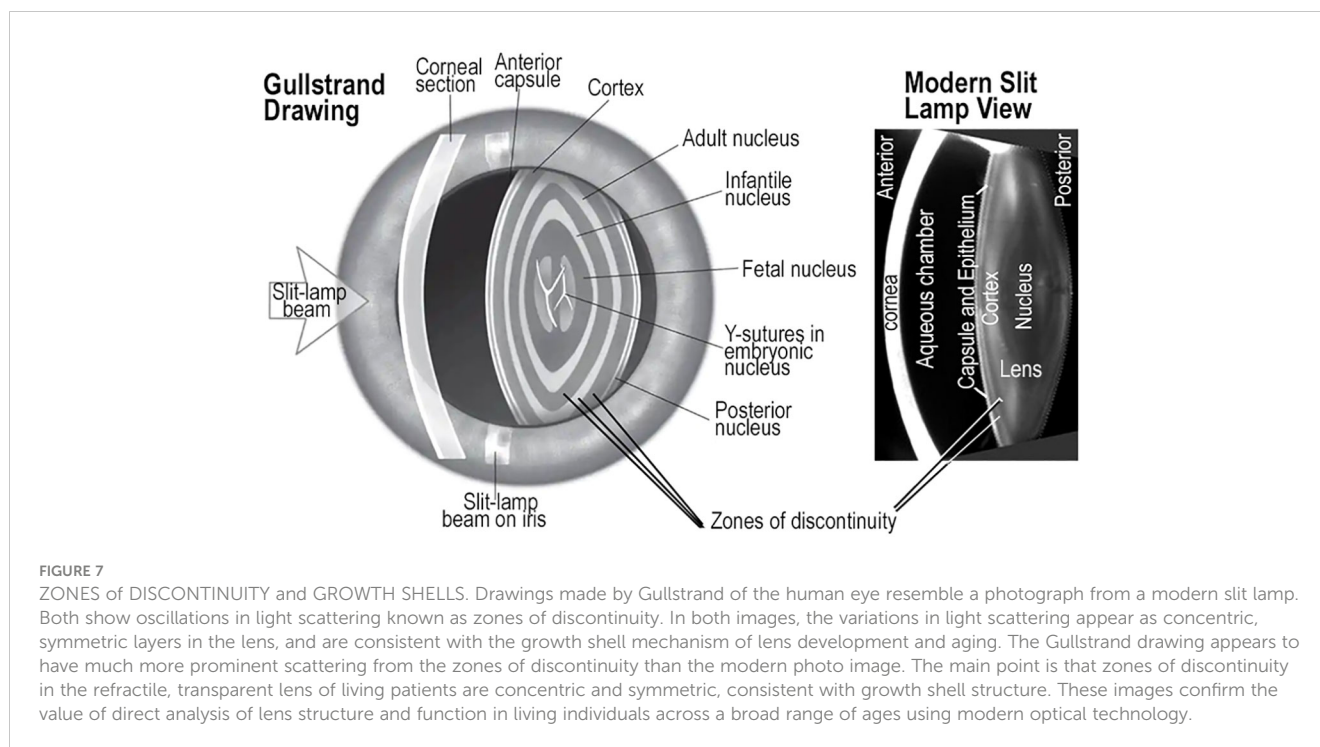
is ordered at all scales of structure, from molecules to the whole tissue, the "crystalline" biological lens is not crystalline. It is formed by concentric shells of symmetric lens fibers (Figures 2, 4, 6). Complex, synergistic, and cooperative, often overlapping, signaling pathways promote structural and functional longevity of lens function (11, 24) Current research needs to consider interactions within networks of growth factors in the regular and coordinated assembly of new growth shells in the mechanism of lens development.

Discussion

It is important to realize that the radius of curvature of a growth shell is symmetric both anteriorly and posteriorly. The precise dimensions are carefully regulated to maximize the optical function of the biconvex, biological lens. The St fibers attached at the posterior and anterior poles form two spatial organizing centers, separated by the equator, in each growth shell (Figures 4, 6). Posterior to the lens equator, the St fibers orient the SSh fibers to form a posterior convexity, and anterior to the equator the St fibers orient SSh fibers to form an anterior convexity. The focal point of a biconvex lens depends on the symmetric gradient in the index of refraction, and the curvature of both the anterior and posterior surfaces. While formed by secondary fibers in the peripheral cortex, each GROWTH SHELL is dynamic and plastic. The surface curvatures of the posterior and anterior hemispheres can adjust to the changing optical requirements of image formation during development and growth of the eye (97, 127, 128). As the lens grows, the newest growth shells (Figures 3, 4) are added between the elongating cortical fibers and the deeper established growth shells. Between the deep cortex and the superficial nucleus, new growth shells form a thin layer that can respond and continuously modify the optics of the growing eye. In contrast, fibers in older, deeper growth shells become highly interconnected and stabilized in the nucleus, in what is known as an electrophysiological "syncytium" (17).

It should be emphasized that not all light scattering is the same. Light scattering depends on wavelength, intensity and scattering angle, the index of refraction, the size, shape and concentration of scatterers, their interactions, symmetry, order, and other biophysical parameters including pressure, temperature, and concentration (129–133). The diversity of differentiating cells and fibers generated in growth shells can be evaluated *in vivo* as variations in fiber structure optimize image formation in the human visual system (130, 134–136). The diversity of fibers and the plasticity of growth shells seem to account for the variability observed in the zones of discontinuity (Figure 7) (11, 137, 138). Plasticity can account for sensitivity of differentiating fibers to environmental factors including glucose levels, toxic substances, or osmolytes penetrating the lens through the microcirculation to reach the differentiating lens fibers.

When the layered structure of the lens was first observed *in vivo* by Gullstrand, the inventor of the slit lamp, variations in scattered

FIGURE 7
ZONES of DISCONTINUITY and GROWTH SHELLS. Drawings made by Gullstrand of the human eye resemble a photograph from a modern slit lamp. Both show oscillations in light scattering known as zones of discontinuity. In both images, the variations in light scattering appear as concentric, symmetric layers in the lens, and are consistent with the growth shell mechanism of lens development and aging. The Gullstrand drawing appears to have much more prominent scattering from the zones of discontinuity than the modern photo image. The main point is that zones of discontinuity in the refractile, transparent lens of living patients are concentric and symmetric, consistent with growth shell structure. These images confirm the value of direct analysis of lens structure and function in living individuals across a broad range of ages using modern optical technology.

light established the basis for understanding the concentric growth shells. Their symmetry, refraction, and transparency could be observed directly in the human lens (Figure 7) (139). Small fluctuations in refractive index gradient and non-random scattering are associated with normal growth and development resulting from modified apoptosis, mitophagy, or autophagocytosis (136, 140–142). These mechanisms are commonly associated with cell death and cell replacement, not prolongation of molecular and cellular longevity, typical of the biological lens (143, 144). In a healthy eye, small fluctuations in the refractive index that produce light scattering from zones of discontinuity, do not impair vision (145) (Figure 7). Detailed computer aided drawings of differentiating lens fibers in normal growth shells can explain images commonly recorded in slit lamp examinations (22, 36–38, 41, 65). In a growth shell, decreasing oxidative metabolism results in the loss of organelles and the reduction in reactive oxygen species to improve transparency during growth of the lens. In fact, all primary and secondary fibers formed in a lens are retained for a lifetime. Lens fiber differentiation involves unique protective mechanisms including antioxidants, microcirculation, cytoskeletal stability, post-translational modification (PTM), and high levels of small heat shock proteins (sHSP) to enhance optical function (symmetry, GRIN, and transparency) of a lens (11). Failure to preserve the viability of any fiber is presumed to lead to pathology. Typical lens fiber differentiation, occurring during lens growth, seeks to decrease the dimensions of irregularities in the refractive index, "n", well below micron sizes. The subtle light scattering from tiny, often temporal, spatial fluctuations in "n", is known as Rayleigh scattering. These tiny fluctuations in "n" are not readily observed histologically, even in electron micrographs (130, 133, 146, 147). While changes in Rayleigh scattering can be a measure of differentiation of normal transparent subcellular structure in living animals, it can also be predictive of the progressive loss of transparency under unfavorable conditions of molecular and cellular aging (11, 91, 92, 130–132, 148, 149).

Conclusion

The human lens is not glass, but could be, if nature chose a developmental mechanism different than growth shells. Other ectodermal derivatives in the integument are dehydrated, including hair, nails, feathers, and claws. Dehydration of the fibers of the developed lens is all that is needed to produce a solid, glass-like lens, similar to a camera lens. For example, when a lens is removed from an eye (rodent, cat, dog, zebrafish, other) and allowed to dehydrate slowly, in a controlled laboratory environment, a biological lens can transition into a transparent, refractile solid. Instead, nature chose to (bio)engineer a highly symmetric and interconnected growth shell system of lens fibers, supported by an unusual microcirculation that limits oxidative metabolism and conserves hydration, physiological homeostasis, and uniform nourishment in a cellular lens. In a biological lens, optical function is prolonged in the visual system over a lifetime (7, 30, 31, 47, 56). A relevant comparison can be made between hydration in a lens and the tardigrade, an extremotolerant organism known to be able to maintain its cellular structure under conditions of complete dehydration (anhydrobiosis) (150). Similarly, the fiber structure of a lens must be maintained under conditions of severe dehydration. While there are advantages to conducting research on biological lenses from a materials science perspective, human vision demands more than a piece of glass or plastic. The symmetry of the growth shells not only prolongs the functional life of a lens, it supports dynamic modifications that optimize the optics of the visual system. The growth shell microcirculation is a major physiological innovation. The vascular system in non-lens tissue

consists of lymphatics and blood vessels that supply oxygen and nutrients to cells. The vasculature modulates cell and tissue fluid homeostasis. In a lens, oxygen is toxic and lymphatics carry immune cells that can recognize modified, aging cells, like the lens fibers, as abnormal and destroy them. In growth shells, the microcirculation is a natural alternative to the typical systemic vasculature. The growth shell microcirculation regulates hydration and provides nutrition in a protective environment of antioxidants and stress response proteins, to optimize cellular, molecular, and functional longevity of refractile, transparent lens fibers.

Coordinated, synchronous differentiation of lens fibers in growth shells is necessary for the optics of the human eye to adjust as the visual system grows and ages. Even though multiple levels of protection (including post-translation modifications, antioxidants, and small heat shock proteins) prolong the biological lens for an unusually long functional life, tiny failures at the molecular level and multifactorial, submicroscopic events can slowly and progressively accumulate and disrupt symmetry and order until a "tipping" point is reached (11, 151–154). The greatest risk factor for loss of transparency is aging of molecular and cellular constituents (11, 24). Membrane specializations (projections, protrusions and connections) between fiber cells change with normal lens development and are associated with formation of the symmetric growth shells. Specific surface features characterizing the boundary of the organelle free zone (OFZ), are not well defined in a normal lens. In abnormal lenses, where fiber differentiation is disrupted, the symmetric relationship(s) between straight and S-shaped fibers in growth shells is distorted, and result in an asymmetric pattern of sutures. (22,37,38). Advances in imaging and analytical sciences suggest that novel integrated research on lens symmetry, GRIN, and transparency in growth shells, will improve our knowledge of natural protection for the optics of individuals at risk for lens opacification that accounts for more than 50% of vision impairment globally (58, 130, 133, 155–157).

Publisher's note

All claims expressed in this article are solely those of the authors and do not necessarily represent those of their affiliated organizations, or those of the publisher, the editors and the reviewers. Any product that may be evaluated in this article, or claim that may be made by its manufacturer, is not guaranteed or endorsed by the publisher.

References

1. Augusteyn RC. Growth of the eye lens: I. Weight accumulation in multiple species. *Mol Vis*. (2014) 20:410–26.

2. Bassnett S, Sikic H. The lens growth process. *Prog Retin Eye Res*. (2017) 60:181–200. doi: 10.1016/j.preteyeres.2017.04.001

3. Cvekl A, Ashery-Padan R. The cellular and molecular mechanisms of vertebrate lens development. *Development*. (2014) 141:4432–47. doi: 10.1242/dev.107953

4. Sjodal M, Edlund T, Gunhaga L. Time of exposure to BMP signals plays a key role in the specification of the olfactory and lens placodes ex vivo. *Dev Cell*. (2007) 13:141–9. doi: 10.1016/j.devcel.2007.04.020

5. Grocott T, Tambalo M, Streit A. The peripheral sensory nervous system in the vertebrate head: a gene regulatory perspective. *Dev Biol*. (2012) 370:3–23. doi: 10.1016/j.ydbio.2012.06.028

6. Schlosser G. Vertebrate cranial placodes as evolutionary innovations–the ancestor's tale. *Curr Top Dev Biol*. (2015) 111:235–300. doi: 10.1016/bs.ctdb.2014.11.008

7. Giannone AA, Li L, Sellitto C, White TW. Physiological mechanisms regulating lens transport. *Front Physiol*. (2021) 12:818649. doi: 10.3389/fphys.2021.818649

8. Greiling TM, Clark JI. New insights into the mechanism of lens development using zebra fish. *Int Rev Cell Mol Biol*. (2012) 296:1–61. doi: 10.1016/B978-0-12-394307-1.00001-1

9. Cvekl A, McGreal R, Liu W. Lens development and crystallin gene expression. *Prog Mol Biol Transl Sci*. (2015) 134:129–67. doi: 10.1016/bs.pmbts.2015.05.001

10. Cvekl A, Zhang X. Signaling and gene regulatory networks in mammalian lens development. *Trends Genet*. (2017) 33:677–702. doi: 10.1016/j.tig.2017.08.001

11. Quinlan RA, Clark JI. Insights into the biochemical and biophysical mechanisms mediating the longevity of the transparent optics of the eye lens. *J Biol Chem.* (2022) 298:102537. doi: 10.1016/j.jbc.2022.102537

12. Beebe DC. Maintaining transparency: a review of the developmental physiology and pathophysiology of two avascular tissues. *Semin Cell Dev Biol.* (2008) 19:125–33. doi: 10.1016/j.semcdb.2007.08.014

13. Brown NP, Brown AJ. *Lens Disorders: A Clinical Manual of Cataract Diagnosis.* Oxford, U.K: Butterworth-Heinemann Ltd (1996).

14. Lovicu FJ, Robinson ML. *Development of the Ocular Lens.* Cambridge, U.K: Cambridge University Press (2004). doi: 10.1017/CBO9780511529825

15. Nowak RB, Fischer RS, Zoltoski RK, Kuszak JR, Fowler VM. Tropomodulin1 is required for membrane skeleton organization and hexagonal geometry of fiber cells in the mouse lens. *J Cell Biol.* (2009) 186:915–28. doi: 10.1083/jcb.200905065

16. Brown NP, Koretz JF, Bron AJ. The development and maintenance of emmetropia. *Eye (Lond).* (1999) 13:83–92. doi: 10.1038/eye.1999.16

17. Shi Y, Barton K, Maria A, Petrash JM, Shiels A, Bassnett S. The stratified syncytium of the vertebrate lens. *J Cell Sci.* (2009) 122:1607–15. doi: 10.1242/jcs.045203

18. Sikic H, Shi Y, Lubura S, Bassnett S. A full lifespan model of vertebrate lens growth. *R Soc Open Sci.* (2017) 4:160695. doi: 10.1098/rsos.160695

19. Oyster CW. *The Human Eye.* Sunderland, MA, USA: Sinauer Associates (1999).

20. Worgul BV. "Lens". In: Jakobiec F, editor. *Ocular anatomy, embryology and teratology.* Philadelphia: Harper & Row (1982). p. 355–89.

21. Muralidharan G, Martinez-Enriquez E, Birkenfeld J, Velasco-Ocana M, Perez-Merino P, Marcos S. Morphological changes of human crystalline lens in myopia. *BioMed Opt Express.* (2019) 10:6084–95. doi: 10.1364/BOE.10.006084

22. Kuszak JR, Zoltoski RK, Tiedemann CE. Development of lens sutures. *Int J Dev Biol.* (2004) 48:889–902. doi: 10.1387/ijdb.041880jk

23. Cheng C, Wang K, Hoshino M, Uesugi K, Yagi N, Pierscionek B. EphA2 affects development of the eye lens nucleus and the gradient of refractive index. *Invest Ophthalmol Vis Sci.* (2022) 63:2. doi: 10.1167/iovs.63.1.2

24. Clark JI. Biology of the transparent lens and changes with age. In: Albert JMD, Azar D, Young LH, editors. *Albert and Jakobiec's Principles and Practice of Ophthalmology.* Springer, Cham, Switzerland (2021). p. 188–201.

25. Schachar RA. Central surface curvatures of postmortem- extracted intact human crystalline lenses: implications for understanding the mechanism of accommodation. *Ophthalmology.* (2004) 111:1699–704. doi: 10.1016/S0161-6420(04)00669-4

26. Brown N. The change in lens curvature with age. *Exp Eye Res.* (1974) 19:175–83. doi: 10.1016/0014-4835(74)90034-7

27. Marcos S, Martinez-Enriquez E, Vinas M, Castro A, Dorronsoro C, Bang SP, et al. Simulating outcomes of cataract surgery: important advances in ophthalmology. *Annu Rev BioMed Eng.* (2021) 23:277–306. doi: 10.1146/annurev-bioeng-082420-035827

28. Marcos S, Werner JS, Burns SA, Merigan WH, Artal P, Atchison DA, et al. Vision science and adaptive optics, the state of the field. *Vision Res.* (2017) 132:3–33. doi: 10.1016/j.visres.2017.01.006

29. Cheng C, Fowler VM, Gong X. EphA2 and ephrin-A5 are not a receptor-ligand pair in the ocular lens. *Exp Eye Res.* (2017) 162:9–17. doi: 10.1016/j.exer.2017.06.016

30. Bassnett S, Shi Y, Vrensen GF. Biological glass: structural determinants of eye lens transparency. *Philos Trans R Soc Lond B Biol Sci.* (2011) 366:1250–64. doi: 10.1098/rstb.2010.0302

31. Donaldson PJ, Grey AC, Maceo Heilman B, Lim JC, Vaghefi E. The physiological optics of the lens. *Prog Retin Eye Res.* (2017) 56:e1–e24. doi: 10.1016/j.preteyeres.2016.09.002

32. Pierscionek BK, Regini JW. The gradient index lens of the eye: an opto-biological synchrony. *Prog Retin Eye Res.* (2012) 31:332–49. doi: 10.1016/j.preteyeres.2012.03.001

33. Wang K, Pu Y, Chen L, Hoshino M, Uesugi K, Yagi N, et al. Optical development in the zebrafish eye lens. *FASEB J.* (2020) 34:5552–62. doi: 10.1096/fj.201902607R

34. Cheng C, Nowak RB, Gao J, Sun X, Biswas SK, Lo WK, et al. Lens ion homeostasis relies on the assembly and/or stability of large connexin 46 gap junction plaques on the broad sides of differentiating fiber cells. *Am J Physiol Cell Physiol.* (2015) 308:C835–47. doi: 10.1152/ajpcell.00372.2014

35. Cheng C, Parreno J, Nowak RB, Biswas SK, Wang K, Hoshino M, et al. Age-related changes in eye lens biomechanics, morphology, refractive index and transparency. *Aging (Albany NY).* (2019) 11:12497–531. doi: 10.18632/aging.v11i24

36. Kuszak JR, Mazurkiewicz M, Jison L, Madurski A, Ngando A, Zoltoski RK. Quantitative analysis of animal model lens anatomy: accommodative range is related to fiber structure and organization. *Vet Ophthalmol.* (2006) 9:266–80. doi: 10.1111/j.1463-5224.2006.00506.x

37. Kuszak JR, Mazurkiewicz M, Zoltoski R. Computer modeling of secondary fiber development and growth: I. Nonprimate lenses. *Mol Vis.* (2006) 12:251–70.

38. Kuszak JR, Zoltoski RK, Sivertson C. Fibre cell organization in crystalline lenses. *Exp Eye Res.* (2004) 78:673–87. doi: 10.1016/j.exer.2003.09.016

39. Kuszak JR, Bertram BA, Macsai MS, Rae JL. Sutures of the crystalline lens: a review. *Scan Electron Microsc.* (1984) 3:1369–78.

40. Kuszak JR. The ultrastructure of epithelial and fiber cells in the crystalline lens. *Int Rev Cytol.* (1995) 163:305–50. doi: 10.1016/S0074-7696(08)62213-5

41. Kuszak JR, Novak LA, Brown HG. An ultrastructural analysis of the epithelial-fiber interface (EFI) in primate lenses. *Exp Eye Res.* (1995) 61:579–97. doi: 10.1016/S0014-4835(05)80052-1

42. Donaldson PJ, Petrova RS, Nair N, Chen Y, Schey KL. Regulation of water flow in the ocular lens: new roles for aquaporins. *J Physiol.* (2024) 602:3041–56. doi: 10.1113/JP284102

43. Huxley JS. *Problems of Relative Growth.* New York, N.Y: Dover Publications (1972).

44. Thompson DW. *On Growth and Form. 2nd.* United Kingdom: Cambridge University Press (1917). doi: 10.5962/bhl.title.11332

45. Donaldson PJ, Chen Y, Petrova RS, Grey AC, Lim JC. Regulation of lens water content: Effects on the physiological optics of the lens. *Prog Retin Eye Res.* (2023) 95:101152. doi: 10.1016/j.preteyeres.2022.101152

46. Shahidullah M, Mandal A, Mathias RT, Gao J, Krizaj D, Redmon S, et al. TRPV1 activation stimulates NKCC1 and increases hydrostatic pressure in the mouse lens. *Am J Physiol Cell Physiol.* (2020) 318:C969–80. doi: 10.1152/ajpcell.00391.2019

47. Petrova RS, Nair N, Bavana N, Chen Y, Schey KL, Donaldson PJ. Modulation of membrane trafficking of AQP5 in the lens in response to changes in zonular tension is mediated by the mechanosensitive channel TRPV1. *Int J Mol Sci.* (2023) 24(10):9080. doi: 10.3390/ijms24109080

48. Robinson KR, Patterson JW. Localization of steady currents in the lens. *Curr Eye Res.* (1982) 2:843–7. doi: 10.3109/02713688209020020

49. Gao J, Sun X, Moore LC, White TW, Brink PR, Mathias RT. Lens intracellular hydrostatic pressure is generated by the circulation of sodium and modulated by gap junction coupling. *J Gen Physiol.* (2011) 137:507–20. doi: 10.1085/jgp.201010538

50. Gao J, Sun X, White TW, Delamere NA, Mathias RT. Feedback regulation of intracellular hydrostatic pressure in surface cells of the lens. *Biophys J.* (2015) 109:1830–9. doi: 10.1016/j.bpj.2015.09.018

51. Gao J, Wang H, Sun X, Varadaraj K, Li L, White TW, et al. The effects of age on lens transport. *Invest Ophthalmol Vis Sci.* (2013) 54:7174–87. doi: 10.1167/iovs.13-12593

52. Candia OA, Mathias R, Gerometta R. Fluid circulation determined in the isolated bovine lens. *Invest Ophthalmol Vis Sci.* (2012) 53:7087–96. doi: 10.1167/iovs.12-10295

53. Patterson JW. Characterization of the equatorial current of the lens. *Ophthalmic Res.* (1988) 20:139–42. doi: 10.1159/000266570

54. Chen Y, Petrova RS, Qiu C, Donaldson PJ. Intracellular hydrostatic pressure regulation in the bovine lens: a role in the regulation of lens optics? *Am J Physiol Regul Integr Comp Physiol.* (2022) 322:R263–79. doi: 10.1152/ajpregu.00309.2021

55. Borchman D, Yappert MC. Lipids and the ocular lens. *J Lipid Res.* (2010) 51:2473–88. doi: 10.1194/jlr.R004119

56. Donaldson PJ, Musil LS, Mathias RT. Point: A critical appraisal of the lens circulation model–an experimental paradigm for understanding the maintenance of lens transparency? *Invest Ophthalmol Vis Sci.* (2010) 51:2303–6. doi: 10.1167/iovs.10-5350

57. Delamere NA, Shahidullah M, Mathias RT, Gao J, Sun X, Sellitto C, et al. Signaling between TRPV1/TRPV4 and intracellular hydrostatic pressure in the mouse lens. *Invest Ophthalmol Vis Sci.* (2020) 61:58. doi: 10.1167/iovs.61.6.58

58. Schey KL, Gletten RB, O'Neale CVT, Wang Z, Petrova RS, Donaldson PJ. Lens aquaporins in health and disease: location is everything! *Front Physiol.* (2022) 13:882550. doi: 10.3389/fphys.2022.882550

59. Zelenka PS. Regulation of cell adhesion and migration in lens development. *Int J Dev Biol.* (2004) 48:857–65. doi: 10.1387/ijdb.041871pz

60. Cheng C, Nowak RB, Biswas SK, Lo WK, FitzGerald PG, Fowler et al. VM. Tropomodulin 1 regulation of actin is required for the formation of large paddle protrusions between mature lens fiber cells. *Invest Ophthalmol Vis Sci.* (2016) 57:4084–99. doi: 10.1167/iovs.16-19949

61. Cheng C, Nowak RB, Fowler VM. The lens actin filament cytoskeleton: Diverse structures for complex functions. *Exp Eye Res.* (2017) 156:58–71. doi: 10.1016/j.exer.2016.03.005

62. Ramaekers FC, Osborn M, Schmid E, Weber K, Bloemendal H, Franke WW. Identification of the cytoskeletal proteins in lens-forming cells, a special epitheloid cell type. *Exp Cell Res.* (1980) 127:309–27. doi: 10.1016/0014-4827(80)90437-1

63. Dubbelman M, van der Heijde GL, Weeber HA, G.F. Vrensen. Changes in the internal structure of the human crystalline lens with age and accommodation. *Vision Res.* (2003) 43:2363–75. doi: 10.1016/S0042-6989(03)00428-0

64. Cvekl A, Camerino MJ. Generation of lens progenitor cells and lentoid bodies from pluripotent stem cells: novel tools for human lens development and ocular disease etiology. *Cells.* (2022) 11(21):3516. doi: 10.3390/cells11213516

65. Al-Ghoul KJ, Lane CW, Taylor VL, Fowler WC, Costello MJ. Distribution and type of morphological damage in human nuclear age-related cataracts. *Exp Eye Res.* (1996) 62:237–51. doi: 10.1006/exer.1996.0029

66. Gong X, Cheng C, Xia CH. Connexins in lens development and cataractogenesis. *J Membr Biol.* (2007) 218:9–12. doi: 10.1007/s00232-007-9033-0

67. FitzGerald PG. Lens intermediate filaments. *Exp Eye Res.* (2009) 88:165–72. doi: 10.1016/j.exer.2008.11.007

68. Song S, Landsbury A, Dahm R, Liu Y, Zhang Q, Quinlan RA. Functions of the intermediate filament cytoskeleton in the eye lens. *J Clin Invest.* (2009) 119:1837–48. doi: 10.1172/JCI38277

69. Beyer EC, Berthoud VM. Connexin hemichannels in the lens. *Front Physiol*. (2014) 5:20. doi: 10.3389/fphys.2014.00020

70. Audette DS, Scheiblin DA, Duncan MK. The molecular mechanisms underlying lens fiber elongation. *Exp Eye Res*. (2017) 156:41–9. doi: 10.1016/j.exer.2016.03.016

71. Rao PV, Maddala R. Ankyrin-B in lens architecture and biomechanics: Just not tethering but more. *Bioarchitecture*. (2016) 6:39–45. doi: 10.1080/19490992.2016.1156284

72. Quinlan RA, Sandilands A, Procter JE, Prescott AR, Hutcheson AM, Dahm R, et al. The eye lens cytoskeleton. *Eye (Lond)*. (1999) 13:409–16. doi: 10.1038/eye.1999.115

73. Prescott AR, Sandilands A, Hutcheson AM, Carter JM, Quinlan RA. The intermediate filament cytoskeleton of the lens: an ever changing network through development and differentiation. A minireview. *Ophthalmic Res*. (1996) 28 Suppl 1:58–61.

74. Ireland M, Maisel H, Bradley RH. The rabbit lens cytoskeletal: an ultrastructural analysis. *Ophthalmic Res*. (1978) 10:231–6. doi: 10.1159/000264960

75. Maisel H, Harding CV, Alcala JR, Kuszak J, Bradley R. Morphology of the lens. In: Bloemendal H, editor. *Molecular and cellular biology of the eye lens*. Wiley and Sons, New York (1981). p. 49–84.

76. Simitian G, Virumbrales-Muñoz M, Sánchez de Diego C, Beebe DJ, Kosoff D. Microfluidics in vascular biology research: a critical review for engineers, biologists, and clinicians. *Lab Chip*. (2022) 22:3618–36. doi: 10.1039/D2LC00352J

77. Beebe DJ, Mensing GA, Walker GM. Physics and applications of microfluidics in biology. *Annu Rev BioMed Eng*. (2002) 4:261–86. doi: 10.1146/annurev.bioeng.4.112601.125916

78. Walker GM, Zeringue HC, Beebe DJ. Microenvironment design considerations for cellular scale studies. *Lab Chip*. (2004) 4:91–7. doi: 10.1039/b311214d

79. Sackmann EK, Fulton AL, Beebe DJ. The present and future role of microfluidics in biomedical research. *Nature*. (2014) 507:181–9. doi: 10.1038/nature13118

80. Fialova S, Pochylý F, Kotek M, Jašíková D. Velocity profiles of fluid flow close to a hydrophobic surface. *EPJ Web Conferences*. (2017) 143:02023. doi: 10.1051/epjconf/201714302023

81. Moller MN, Li Q, Chinnaraj M, Cheung HC, Lancaster JR Jr., Denicola A. Solubility and diffusion of oxygen in phospholipid membranes. *Biochim Biophys Acta*. (2016) 1858:2923–30. doi: 10.1016/j.bbamem.2016.09.003

82. Subczynski WK, Widomska J, Mainali L. Factors determining the oxygen permeability of biological membranes: oxygen transport across eye lens fiber-cell plasma membranes. *Adv Exp Med Biol*. (2017) 977:27–34. doi: 10.1007/978-3-319-55231-6

83. Bernecker C, Kofeler H, Pabst G, Trotzmuller M, Kolb D, Strohmayer K, et al. Cholesterol deficiency causes impaired osmotic stability of cultured red blood cells. *Front Physiol*. (2019) 10:1529. doi: 10.3389/fphys.2019.01529

84. Widomska J, Subczynski WK, Mainali L, Raguz M. Cholesterol bilayer domains in the eye lens health: A review. *Cell Biochem Biophys*. (2017) 75:387–98. doi: 10.1007/s12013-017-0812-7

85. Subczynski WK, Pasenkiewicz-Gierula M, Widomska J, Mainali L, Raguz M. High cholesterol/low cholesterol: effects in biological membranes: A review. *Cell Biochem Biophys*. (2017) 75:369–85. doi: 10.1007/s12013-017-0792-5

86. Subczynski WK, Pasenkiewicz-Gierula M, Widomska J. Protecting the eye lens from oxidative stress through oxygen regulation. *Antioxidants*. (2023) 12(9):1783. doi: 10.3390/antiox12091783

87. Bassnett S, Beebe DC. Coincident loss of mitochondria and nuclei during lens fiber cell differentiation. *Dev Dyn*. (1992) 194:85–93. doi: 10.1002/aja.1001940202

88. Sikic H, Shi Y, Lubura S, Bassnett S. A stochastic model of eye lens growth. *J Theor Biol*. (2015) 376:15–31. doi: 10.1016/j.jtbi.2015.03.021

89. Moncaster JA, Moir RD, Burton MA, Chadwick O, Minaeva O, Alvarez VE, et al. Alzheimer's disease amyloid-beta pathology in the lens of the eye. *Exp Eye Res*. (2022) 221:108974. doi: 10.1016/j.exer.2022.108974

90. Clark JI, Neuringer JR, Benedek GB. Phase separation and lens cell age. *J Gerontol*. (1983) 38:287–92. doi: 10.1093/geronj/38.3.287

91. Latina M, Chylack LT Jr., Fagerholm P, Nishio I, Tanaka T, Palmquist BM. Dynamic light scattering in the intact rabbit lens. Its relation to protein concentration. *Invest Ophthalmol Vis Sci*. (1987) 28:175–83.

92. Nishio I, Weiss JN, Tanaka T, Clark JI, Giblin FJ, Reddy VN, et al. *In vivo* observation of lens protein diffusivity in normal and X-irradiated rabbit lenses. *Exp Eye Res*. (1984) 39:61–8. doi: 10.1016/0014-4835(84)90115-5

93. Klesert TR, Cho DH, Clark JI, Maylie J, Adelman J, Snider L, et al. Mice deficient in Six5 develop cataracts: implications for myotonic dystrophy. *Nat Genet*. (2000) 25:105–9. doi: 10.1038/75490

94. Moncaster JA, Pineda R, Moir RD, Lu S, Burton MA, Ghosh JG, et al. Alzheimer's disease amyloid-beta links lens and brain pathology in Down syndrome. *PloS One*. (2010) 5:e10659. doi: 10.1371/journal.pone.0010659

95. Yuen J, Li Y, Shapiro LG, Clark JI, Arnett E, Sage EH, et al. Automated, computerized, feature-based phenotype analysis of slit lamp images of the mouse lens. *Exp Eye Res*. (2008) 86:562–75. doi: 10.1016/j.exer.2007.11.019

96. Marcos S, Artal P, Atchison DA, Hampson K, Legras R, Lundstrom L, et al. Adaptive optics visual simulators: a review of recent optical designs and applications [Invited]. *BioMed Opt Express*. (2022) 13:6508–32. doi: 10.1364/BOE.473458

97. Kroger RH. Optical plasticity in fish lenses. *Prog Retin Eye Res*. (2013) 34:78–88. doi: 10.1016/j.preteyeres.2012.12.001

98. Coulombre AJ, Herrmann H. Lens development. 3. Relationship between the growth of the lens and the growth of the outer eye coat. *Exp Eye Res*. (1965) 4:302–11. doi: 10.1016/S0014-4835(65)80045-8

99. Yamamoto Y. Growth of lens and ocular environment: role of neural retina in the growth of mouse lens as revealed by an implantation experiment. *Dev Growth Differ*. (1976) 18:273–8. doi: 10.1111/j.1440-169X.1976.00273.x

100. Aose M, Linbo TH, Lawrence O, Senoo T, Raible DW, Clark JI. The occhiolino (occ) mutant Zebrafish, a model for development of the optical function in the biological lens. *Dev Dyn*. (2017) 246:915–24. doi: 10.1002/dvdy.24511

101. Sivak JG. Optics of the eye of the "four-eyed fish" (Anableps anableps). *Vision Res*. (1976) 16:531–4. doi: 10.1016/0042-6989(76)90035-3

102. Perez LN, Lorena J, Costa CM, Araujo MS, Frota-Lima GN, Matos-Rodrigues GE, et al. Eye development in the four-eyed fish Anableps: cranial and retinal adaptations to simultaneous aerial and aquatic vision. *Proc R Soc B Biol Sci*. (2017) 284(1852):20170157. doi: 10.1098/rspb.2017.0157

103. Kanungo J, Swamynathan SK, Piatigorsky J. Abundant corneal gelsolin in Zebrafish and the 'four-eyed' fish, Anableps: possible analogy with multifunctional lens crystallins. *Exp Eye Res*. (2004) 79:949–56. doi: 10.1016/j.exer.2004.04.002

104. Schartau JM, Sjogreen B, Gagnon YL, Kroger RH. Optical plasticity in the crystalline lenses of the cichlid fish Aequidens pulcher. *Curr Biol*. (2009) 19:122–6. doi: 10.1016/j.cub.2008.11.062

105. Beebe D, Garcia C, Wang X, Rajagopal R, Feldmeier M, Kim JY, et al. Contributions by members of the TGFbeta superfamily to lens development. *Int J Dev Biol*. (2004) 48:845–56. doi: 10.1387/ijdb.041869db

106. Brewitt B, Clark JI. Growth and transparency in the lens, an epithelial tissue, stimulated by pulses of PDGF. *Science*. (1988) 242:777–9. doi: 10.1126/science.3187521

107. Cheng C. EphA2 and ephrin-A5 guide eye lens suture alignment and influence whole lens resilience. *Invest Ophthalmol Vis Sci*. (2021) 62:3. doi: 10.1167/iovs.62.15.3

108. Faber SC, Dimanlig P, Makarenkova HP, Shirke S, Ko K, Lang RA. Fgf receptor signaling plays a role in lens induction. *Development*. (2001) 128:4425–38. doi: 10.1242/dev.128.22.4425

109. Lovicu FJ, McAvoy JW. Growth factor regulation of lens development. *Dev Biol*. (2005) 280:1–14. doi: 10.1016/j.ydbio.2005.01.020

110. McAvoy JW, Chamberlain CG, de Iongh RU, Hales and F.J. Lovicu AM. Peter Bishop Lecture: growth factors in lens development and cataract: key roles for fibroblast growth factor and TGF-beta. *Clin Exp Ophthalmol*. (2000) 28:133–9. doi: 10.1046/j.1442-9071.2000.00310.x

111. McAvoy JW, Dawes LJ, Sugiyama Y, Lovicu FJ. Intrinsic and extrinsic regulatory mechanisms are required to form and maintain a lens of the correct size and shape. *Exp Eye Res*. (2017) 156:34–40. doi: 10.1016/j.exer.2016.04.009

112. Reneker LW, Overbeek PA. Lens-specific expression of PDGF-A alters lens growth and development. *Dev Biol*. (1996) 180:554–65. doi: 10.1006/dbio.1996.0328

113. Lovicu FJ, McAvoy JW, de Iongh RU. Understanding the role of growth factors in embryonic development: insights from the lens. *Philos Trans R Soc Lond B Biol Sci*. (2011) 366:1204–18. doi: 10.1098/rstb.2010.0339

114. Li H, Mao Y, Bouaziz M, Yu H, Qu X, Wang F, et al. Lens differentiation is controlled by the balance between PDGF and FGF signaling. *PloS Biol*. (2019) 17:e3000133. doi: 10.1371/journal.pbio.3000133

115. Schatteman GC, Motley ST, Effmann EL, Bowen-Pope DF. Platelet-derived growth factor receptor alpha subunit deleted Patch mouse exhibits severe cardiovascular dysmorphogenesis. *Teratology*. (1995) 51:351–66. doi: 10.1002/tera.1420510602

116. Cvekl A, Eliscovich C. Crystallin gene expression: Insights from studies of transcriptional bursting. *Exp Eye Res*. (2021) 207:108564. doi: 10.1016/j.exer.2021.108564

117. Cheng C, Gao J, Sun X, Mathias RT. Eph-ephrin signaling affects eye lens fiber cell intracellular voltage and membrane conductance. *Front Physiol*. (2021) 12:772276. doi: 10.3389/fphys.2021.772276

118. Zhou Y, Bennett TM, Ruzycki PA, Shiels A. Mutation of the EPHA2 tyrosine-kinase domain dysregulates cell pattern formation and cytoskeletal gene expression in the lens. *Cells*. (2021) 10(10):2606. doi: 10.3390/cells10102606

119. Brewitt B, Clark JI. A new method for study of normal lens development *in vitro* using pulsatile delivery of PDGF or EGF in HL-1 serum-free medium. *Vitro Cell Dev Biol*. (1990) 26:305–14. doi: 10.1007/BF02624462

120. Brewitt B, Talian JC, Zelenka PS. Cell cycle synchrony in the developing chicken lens epithelium. *Dev Biol*. (1992) 152:315–22. doi: 10.1016/0012-1606(92)90138-7

121. Brewitt B, Teller DC, Clark JI. Periods of oscillatory growth in developing ocular lens correspond with cell cycle times. *J Cell Physiol*. (1992) 150:586–92. doi: 10.1002/jcp.1041500320

122. Wang D, Wang E, Liu K, Xia CH, Li S, Gong X. Roles of TGFbeta and FGF signals during growth and differentiation of mouse lens epithelial cell *in vitro*. *Sci Rep*. (2017) 7:7274. doi: 10.1038/s41598-017-07619-5

123. Liu Z, Wang R, Lin H, Liu Y. Lens regeneration in humans: using regenerative potential for tissue repairing. *Ann Transl Med*. (2020) 8:1544. doi: 10.21037/atm

124. Wang Q, McAvoy JW, Lovicu FJ. Growth factor signaling in vitreous humor-induced lens fiber differentiation. *Invest Ophthalmol Vis Sci*. (2010) 51:3599–610. doi: 10.1167/iovs.09-4797

125. Griep AE. Cell cycle regulation in the developing lens. *Semin Cell Dev Biol*. (2006) 17:686–97. doi: 10.1016/j.semcdb.2006.10.004

126. Potts JD, Bassnett S, Kornacker S, Beebe DC. Expression of platelet-derived growth factor receptors in the developing chicken lens. *Invest Ophthalmol Vis Sci*. (1994) 35:3413–21.

127. Wang K, Pierscionek BK. Biomechanics of the human lens and accommodative system: Functional relevance to physiological states. *Prog Retin Eye Res*. (2019) 71:114–31. doi: 10.1016/j.preteyeres.2018.11.004

128. Wang K, Venetsanos DT, Hoshino M, Uesugi K, Yagi N, Pierscionek BK. A modeling approach for investigating opto-mechanical relationships in the human eye lens. *IEEE Trans BioMed Eng*. (2020) 67:999–1006. doi: 10.1109/TBME.10

129. Johnsen S, Widder EA. The physical basis of transparency in biological tissue: ultrastructure and the minimization of light scattering. *J Theor Biol*. (1999) 199:181–98. doi: 10.1006/jtbi.1999.0948

130. Sarangi S, Minaeva O, Ledoux DM, Parsons DS, Moncaster JA, Black CA, et al. *In vivo* quasi-elastic light scattering detects molecular changes in the lenses of adolescents with Down syndrome. *Exp Eye Res*. (2024) 241:109818. doi: 10.1016/j.exer.2024.109818

131. Thurston GM, Hayden DL, Burrows P, Clark JI, Taret VG, Kandel J, et al. Quasielastic light scattering study of the living human lens as a function of age. *Curr Eye Res*. (1997) 16:197–207. doi: 10.1076/ceyr.16.3.197.15410

132. Bettelheim FA. Light scattering in lens research: an essay on accomplishments and promises. *Exp Eye Res*. (2004) 79:747–52. doi: 10.1016/j.exer.2004.06.004

133. Benedek GB, Pande J, Thurston GM, Clark JI. Theoretical and experimental basis for the inhibition of cataract. *Prog Retin Eye Res*. (1999) 18:391–402. doi: 10.1016/S1350-9462(98)00023-8

134. Greiling TM, Clark JI. Early lens development in the zebrafish: a three-dimensional time-lapse analysis. *Dev Dyn*. (2009) 238:2254–65. doi: 10.1002/dvdy.21997

135. Muchowski PJ, Ramsden R, Nguyen Q, Arnett EE, Greiling TM, Anderson SK, et al. Noninvasive measurement of protein aggregation by mutant huntingtin fragments or alpha-synuclein in the lens. *J Biol Chem*. (2008) 283:6330–6. doi: 10.1074/jbc.M709678200

136. Seeberger TM, Matsumoto Y, Alizadeh A, Fitzgerald PG, Clark JI. Digital image capture and quantification of subtle lens opacities in rodents. *J BioMed Opt*. (2004) 9:116–20. doi: 10.1117/1.1630034

137. Koretz JF, Cook CA, Kaufman PL. Aging of the human lens: changes in lens shape at zero-diopter accommodation. *J Opt Soc Am A Opt Image Sci Vis*. (2001) 18:265–72. doi: 10.1364/JOSAA.18.000265

138. Koretz JF, Cook CA, Kuszak JR. The zones of discontinuity in the human lens: development and distribution with age. *Vision Res*. (1994) 34:2955–62. doi: 10.1016/0042-6989(94)90267-4

139. Ehinger B, Grzybowski A. Allvar Gullstrand (1862-1930)–the gentleman with the lamp. *Acta Ophthalmol*. (2011) 89:701–8. doi: 10.1111/aos.2011.89.issue-8

140. Brennan L, Costello MJ, Hejtmancik JF, Menko AS, Riazuddin SA, Shiels A. Autophagy requirements for eye lens differentiation and transparency. *Cells*. (2023) 12 (3):475. doi: 10.3390/cells12030475

141. Costello MJ, Brennan LA, Basu S, Chauss D, Mohamed A, Gilliland KO, et al. Autophagy and mitophagy participate in ocular lens organelle degradation. *Exp Eye Res*. (2013) 116:141–50. doi: 10.1016/j.exer.2013.08.017

142. Morishita H, Mizushima N. Autophagy in the lens. *Exp Eye Res*. (2016) 144:22–8. doi: 10.1016/j.exer.2015.08.019

143. Morishita H, Mizushima N. Autophagy and ageing. *Nihon Rinsho*. (2016) 74:1461–6.

144. Morishita H, Mizushima N. Diverse cellular roles of autophagy. *Annu Rev Cell Dev Biol*. (2019) 35:453–75. doi: 10.1146/annurev-cellbio-100818-125300

145. Bahrami M, Hoshino M, Pierscionek B, Yagi N, Regini J, Uesugi K. Optical properties of the lens: an explanation for the zones of discontinuity. *Exp Eye Res*. (2014) 124:93–9. doi: 10.1016/j.exer.2014.05.009

146. Trokel S. The physical basis for transparency of the crystalline lens. *Invest Ophthalmol*. (1962) 1:493–501.

147. Clark JI. Order and disorder in the transparent media of the eye. *Exp Eye Res*. (2004) 78:427–32. doi: 10.1016/j.exer.2003.10.008

148. Tanaka T, Benedek GB. Observation of protein diffusivity in intact human and bovine lenses with application to cataract. *Invest Ophthalmol*. (1975) 14:449–56.

149. Delaye M, Clark JI, Benedek GB. Identification of the scattering elements responsible for lens opacification in cold cataracts. *Biophys J*. (1982) 37:647–56. doi: 10.1016/S0006-3495(21)00384-2

150. Elbein AD. The metabolism of alpha,alpha-trehalose. *Adv Carbohydr Chem Biochem*. (1974) 30:227–56. doi: 10.1016/S0065-2318(08)60266-8

151. Uwineza A, Kalligeraki AA, Hamada N, Jarrin M, Quinlan RA. Cataractogenic load - A concept to study the contribution of ionizing radiation to accelerated aging in the eye lens. *Mutat Res Rev Mutat Res*. (2019) 779:68–81. doi: 10.1016/j.mrrev.2019.02.004

152. Lampi KJ, Fox CB, David LL. Changes in solvent accessibility of wild-type and deamidated betaB2-crystallin following complex formation with alphaA-crystallin. *Exp Eye Res*. (2012) 104:48–58. doi: 10.1016/j.exer.2012.09.001

153. Lampi KJ, Wilmarth PA, Murray MR, David LL. Lens beta-crystallins: the role of deamidation and related modifications in aging and cataract. *Prog Biophys Mol Biol*. (2014) 115:21–31. doi: 10.1016/j.pbiomolbio.2014.02.004

154. Lou MF. Glutathione and glutaredoxin in redox regulation and cell signaling of the lens. *Antioxid (Basel)*. (2022) 11(10):1973. doi: 10.3390/antiox11101973

155. Benedek GB, Clark JI, Serrallach EN, Young C, Mengel L, Sauke T, et al. Light scattering and reversible cataracts in the calf and human lens. *Philos Trans R Soc London Ser A*. (1979) 293:329–40. doi: 10.1098/rsta.1979.0100

156. Fan X, Monnier VM, Whitson J. Lens glutathione homeostasis: Discrepancies and gaps in knowledge standing in the way of novel therapeutic approaches. *Exp Eye Res*. (2017) 156:103–11. doi: 10.1016/j.exer.2016.06.018

157. Quinlan RA. DRUG DISCOVERY. A new dawn for cataracts. *Science*. (2015) 350:636–7. doi: 10.1126/science.aad6303